CASCADE EFFECTS IN LIFETIME MEASUREMENTS[1)]

Burshtein, M.,[2)] Kazantsev, S.,[2)] Rudakova, T.,[2)] Verolainen, Ya.,[2)] St. Petersburg

The cascade effects in the lifetime measurements are discussed. Theoretical study and experiments with the complex τ-metric set up showed that the role of the cascade effects in the delayed coincidence and the Hanle effect experiments are principally different. These cascade peculiarities may be responsible for the data scatter obtained by the different experimental techniques.

I. INTRODUCTION

A host of experimental data on the radiative lifetimes (τ) of excited atomic and ionic states which appeared in the last two decades indicate a constant need for the reliable values of this atomic constant. Many new experimental methods were elaborated and the known techniques were refined to get the most accurate lifetime data which provide important information about atomic physics, plasma physics and astrophysics.

All experimental techniques for the lifetime determination may be divided into three separate groups: spectroscopic methods, temporal decay techniques and coherent methods which reflect the difference of physical principles incorporated in the measurement procedure. Spectroscopic techniques are based on the measurement of the spectral characteristics of radiation of excited particles and usually provide information about the transition probabilities or the oscillator strenghts from which the radiative lifetimes may be obtained. The hook method, the absorbtion technique, the spectral line emission technique and the method of the natural line width belong to the first group. Temporal decay methods, i.e. delayed coincidence, beam-foil, phase shift techniques make use of the temporal characteristics of the decay of population or the zero-order polarization moment ($\varrho^{(0)}$) of a level investigated after the pulse excitation. The coherent methods (Hanle, level-crossing, quantum beats techniques) are connected with the Zeeman coherence or

[1)] Contribution presented at the 8th Symposium on Elementary Processes and Chemical Reaction in Low Temperature Plasma, STARÁ LESNÁ, May 28 – June 1, 1990

[2)] Institute of Physics, St. Petersburg State University, Universitetskaya nab. 7/9, 199034 ST. PETERSBURG, USSR

the polarization moments $\varrho_q^{(\kappa)}$ of the higher orders (κ=1,2) of the upper level of optical transitions. A great deal of the experimental lifetimes were obtained by the delayed coincedence technique under the electron impact excitation, the beam-foil and the Hanle techniques [6]. The critical comparison of the lifetimes measured by these methods shows that in a number of cases, i.e. for the $4p$ Ne I, $9s$, $9p$ and $9d$ Cs I states [11] and for some levels of the noble gases [8] the difference of the temporal decay and the Hanle method values exceed significantly the given error limits. These inconsistencies result from the systematic errors inherent to these experimental techniques and are not considered in the resulting values. The radiative cascade transitions to the investigating level caused by the nonselectivity of the electron impact, beam foil or gas discharge types of excitation are known to be the major error source of τ measurements by all the above mentioned methods. By these means, the study of the cascade processes together with the cascade-free techniques elaboration on the basis of the selective laser excitation are the important problems of atomic physics.

The aim of this work is to demostrate the role of the cascade effects in the principally different methods of the life time determination which will facilitate the comparative analysis of errors in different experimental methods and perhaps will shed light on the possible origin of the data scatter. One of the most simple ways to realize it is to perform the delayed coincidence and the Hanle effect measurements in one object under the same conditions. The electron gun producing a beam of monokinetic low-energy electrons is a very simple universal object of the kind which without any changes of construction enables to carry on the delayed coincidence [2] and the Hanle effect measurements [5,8] in one object under the same conditions.

II. THEORY

2.1. Decay curve accounting for cascade transitions

The radiative cascadings to the investigated level are the dominant error source in the delayed coincidence technique under the electron impact excitation. The nonselectivity of the excitation leads to the multiexponential decay of population. Considering the multilevel scheme (Fig. 1) the time dependence of the intensity of the spectral line after the short pulse excitation at the instant $t = 0$ is expressed by

$$I_\lambda = N_k^0(t).h\nu_{ik}A_{ki},$$

where

$$N_k^0(t) = \left[N_k^0(0) - \sum_j \frac{A_{jk} - N_j^0(0)}{\gamma_k - \gamma_j}\right] \exp(-\gamma_k^0 t) + \sum_{j=k+1} N_j^0(0) \frac{A_{jk}}{\gamma_k - \gamma_j} \exp(-\gamma_j^0 t),$$

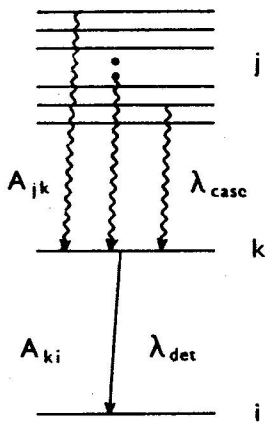

Fig. 1. Multilevel cascade scheme of population.

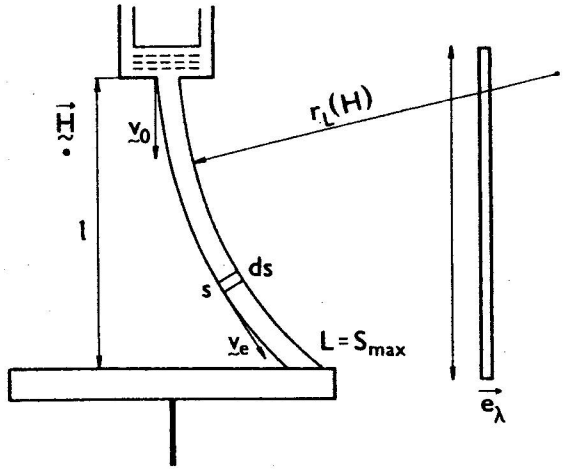

Fig. 2. Scheme of the Hanle effect under low energy electron impact excitation with an account for the curvation of the electron trajectory.

here $N_k^0(0)$ is the initial population of the level k, $\gamma_k^0 = \tau_k^{-1}$ - is the probability of the spontaneous decay of population, A_{jk} - is the probability of the transition from the highly excited level j to the level k, A_{ki} is the probability of the radiative decay of the upper level k, $N_j^0(0)$ - is the initial population of an upper level. The expansion of the function $I_\lambda(t)$ to the exponential components is in a number of cases an incorrect problem which requires information about the scheme of the cascade transitions and the characteristics of the highly excited states (A_{jk},$N_j^0(0)$). As a rule these data are not known and this shortage of information defines one of the major systematic errors of this technique.

2.2. The Hanle signal shape under electron impact excitation

For the most simple and frequently used scheme of the Hanle effect experiment the cascade free signal shape is represented by the Lorentz curve with the width determined by the relaxation constant of coherence of the studied level k. For the case of the cascade transfer of the polarization moments to the studied level k, the Hanle signal shape becomes more complicated. It is represented by a sum of the Lorentz function caused by the direct excitation of the level k and the cascade part which is determined by the atomic constants of all the levels involved in the cascade process [4].

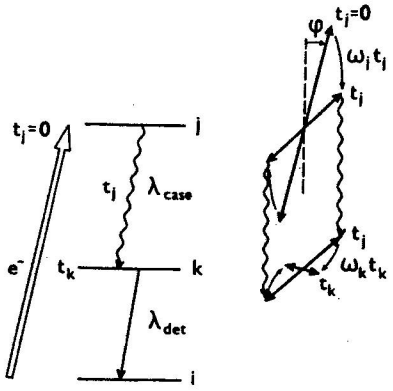

Fig. 3. Classical oscillator model for the cascade Hanle signal shape calculation (b) for the three level scheme (a).

Considering the cascade in the Hanle experiment we shall discuss the peculiarities of the signal shape under low-energy electron beam excitation. The scheme of the experiment is presented in figure 2. The magnetic field is applied to the collision chamber of the electron gun orthogonally to the initial velocity vector of electrons in the beam $\mathbf{v}_0$ and the radiation of a gas in a given spectral line is analysed as a function of the magnetic field strength in the polarization parallel to $\mathbf{v}_0$.

For the three level scheme (Fig. 3a) the cascade signal shape may be obtained using the model of the harmonic oscillator processing in the external magnetic field. We suppose that the electron impact induces the atomic oscillator corresponding to the given electric dipole transition and its oscillation takes place along the velocity vector of the exciting electron $\mathbf{v}_0$. Let at t_j=0 the excitation of the level j occurs, then at the instant t_j the radiative transition to the level k takes place and t_k - is the time interval during which the oscillator $k \rightarrow i$ emits radiation (Fig. 3b). Taking into consideration that the decay constants and the Larmour precession frequencies of the levels j and k are not equal ($\Gamma_k \neq \Gamma_j, \omega_k \neq \omega_j$) the total angle of rotation of the oscillator axis in the external magnetic field will be $\omega_j.t_j + \omega_k.t_k + \varphi$, where φ is the initial phase of the oscillator at the instant t_j=0 (Fig. 3b).

The intensity of the linearly polarized light radiation (e_λ - is the polarization vector) of an ensemble of oscillators in the outer magnetic field H (Fig. 2), taking into consideration the influence of the magnetic field on the electron path in the collision chamber, will take the form [7]:

$$I_{e_\lambda} = I_0 \int_0^L ds \int_0^\infty dt_j e^{-\Gamma_j t_j} \int_0^\infty dt_k e^{-\Gamma_k t_k} \sin^2 \left[\omega_j t_j + \omega_k t_k + \frac{s}{r(H)} \right]$$

here s - is the arc length with the Larmour radius $r(H) = c\sqrt{2m/e}.\sqrt{v}/H$ which corresponds to an electron with the initial energy V, e, m, c - are the electron charge and mass and the light velocity, $L = (\arcsin l/r).r$ - is the total arc length of the curve which represents the electron trajectory in the excitation chamber of an electron gun with the length l (Fig. 2). Calculating the integral (2) we have for the case $l < r$:

$$I_{e_\lambda} = \frac{I_0}{2\Gamma_k \Gamma_j} \left[r.\arcsin\frac{l}{r} + l\sqrt{1 - \frac{l^2}{r^2}} \frac{x_j x_k - 1}{(1+x_j^2)(1+x_k^2)} - \frac{l^2}{r} \frac{x_j + x_k}{(1+x_j^2)(1+x_k^2)} \right] \tag{3}$$

where $x_{j,k} = 2\omega_{j,k}/\Gamma_{j,k}$.

The polarization moment formalism is the most simple way to get the cascade signal shape for the multi-cascade case [4] (Fig. 1). The polarization moment for the sub-ensemble of particles which corresponds to the differential of the arc length ds (Fig. 2) will take the form

$$d_k \rho_q^{(\kappa)} = \sum_{j=1}^{M} (-1)^{J_j + J_k + \kappa + 1} A_{jk} (2J_j + 1) \begin{Bmatrix} J_j & J_j & \kappa \\ J_k & J_k & 1 \end{Bmatrix} \frac{\sum_{q'} D_{qq'}^{(\kappa)} \left[0, \frac{\pi}{2}, \frac{s}{r(H)}\right] T_j^\tau \rho_0^{(\kappa)}}{(\Gamma_j - 2i\omega_j)(\Gamma_k - 2i\omega_k)}.$$

Here M is a number of cascade routes to the level k, J_j, J_k are the momenta of the j and k states, $T_j^\tau \rho_0^{(\kappa)}$ is the polarization moment of the upper state j in the collision frame of reference with the axis directed along the velocity vector of electrons, $D_{qq'}^{(\kappa)} \left[0, \frac{\pi}{2}, \frac{s}{r(H)}\right]$ is the Wigner matrix accounting for the transfer to the laboratory frame of reference.

The total intensity of polarized monochromatic optical radiation gathered from all the collision chamber and caused only by the cascade process will be determined as

$$I_{e_\lambda} = B \int_0^L ds \sum_{\kappa,q} (2\kappa + 1) \begin{Bmatrix} 1 & 1 & \kappa \\ J_k & J_k & J \end{Bmatrix} (-1)^q d_k \rho_k^{(\kappa)} \Phi_{-q}^{(\kappa)}(\mathbf{e}_\lambda),$$

where $\Phi_q^{(\kappa)}(\mathbf{e}_\lambda)$ is the observation tensor with the non-zero components in the laboratory frame of reference expressed as $\Phi_0^{(0)} = -1/\sqrt{3}, \Phi_0^{(2)} = -1/\sqrt{30}, \Phi_2^{(2)} = \Phi_{-2}^{(2)} = 1/2\sqrt{5}$ and B is the numerical constant. Finally for the intensity of the

polarized radiation accounting for the direct and the cascade ways of excitation we have :

$$I_{e_\lambda} = I_{e_\lambda}^{[1]} + I_{e_\lambda}^{[2]},$$

where $I_{e_\lambda}^{[1]}$ is the part of the Hanle signal caused by the direct electron impact excitation of the level k [5,7]:

$$I_{e_\lambda}^{[1]} = a_k.\arcsin\frac{l}{r} + b_k\left(l\sqrt{1-\frac{l^2}{r^2}}\frac{1}{1+\bar{\bar{X}}_k^2} - \frac{l^2}{r}\frac{\bar{\bar{X}}_k}{1+\bar{\bar{X}}_k^2}\right)$$

a_k, b_k - are the quantities proportional to the probabilities of population and the alignment of the level k by the electron impact and the cascade part $I_{e_\lambda}^{[2]}$ is expressed by

$$I_{e_\lambda}^{[2]} = B\sum_{j=1}^{N}(2J_j+1)A_{jk}\left[a_j.r.\arcsin\frac{l}{r} + (-1)^{J_j b_j + I_k + 3}\begin{Bmatrix} J_j & J_j & 2 \\ J_k & J_k & J \end{Bmatrix} L_j\right] \quad (4)$$

where a_j and b_j are the quantities proportional to the probabilities of population and alignment of the level j by the electron impact. L_j is given by

$$L_j = l\sqrt{1-\frac{l^2}{r^2}}\frac{\bar{\bar{X}}_j\bar{\bar{X}}_k - 1}{(1+\bar{\bar{X}}_j^2)(1+\bar{\bar{X}}_k^2)} - \frac{l^2}{r}\frac{\bar{\bar{X}}_j + \bar{\bar{X}}_k}{(1+\bar{\bar{X}}_j^2)(1+\bar{\bar{X}}_k^2)}.$$

2.3. Comparative role of the cascade effect in the delayed coincidence and the Hanle methods

The peculiarities of the cascade effect in the delayed coincidence and the Hanle technique may be analysed using the formulae (1) and (4). The cascade part of the Hanle signal $I_{e_\lambda}^{[2]}$ is the sum of components describing the cascade channels of the studied level k. The sign of every component is determined by the momenta of the upper and lower states. Hence for many cascade transitions from the upper levels with different moments the magnitude of the cascade part of the Hanle signal $I_{e_\lambda}^{[2]}$ may be small in comparison with $I_{e_\lambda}^{[1]}$. The decay curve in the delayed coincidence method for the multicascade case is always represented by a sum of many cascade contributions with the same sign (I). The resolution of this decay curve into different exponents is often an incorrect problem which brings systematic errors to the resulting value of τ_k. Only for the small number of cascade transitions the accuracy of the decay curve expansion may be rather high and the reliable information on γ_j and $\varrho^{(0)}(0)$. A_{jk} may be obtained.

On the other hand the cascade part of the Hanle signal for a small number of cascade routes may be sufficient and will cause uncertainties in the lifetime determination. It is because of these cascade features that the simultaneous use of these two methods appears to be advisable. This complex approach will enable to investigate in detail the characteristics of the delayed coincidence and the Hanle signal shapes which will facilitate the accounting cascade errors.

III. EXPERIMENTAL PROCEDURE

The scheme of the complex τ-metric experimental set-up is given in figure 4. Atoms were excited in the collision chamber of the electron gun (I) generating a collimated electron beam with the average electron current density of 1 - 10 mA/cm^2 and the energy straggling of electrons was not much more than 1 eV. The electron gun consisted of the indirectly heated oxide cathode, three grid anodes and a collector, mounted in a glass bulb. The electron impact excitation was inside the collision chamber with the length of 1-2 cm which was between the third grid and the collector. The electron gun was connected with the vacuum system and was filled with noble gases of spectral purity. The pressure was measured by the McLeod gauge. Light from all the collision chambers was projected on the entrance slit of the grating monochromator (2) orthogonally to the electron beam. Thus the electron beam axis was parallel to the entrance slit of the monochromator. The grating monochromator selected the investigated spectral line which was detected by the photon counting scheme with the help of the photomultiplier PEM-79 (3). The signal from the photomultiplier was amplified by the broad band amplifier (4) and entered the discriminator (5) with the dead time of 80 nsec.

The temporal analysis of radiation by the complex experimental set-up was performed using the delayed coincidence principle. The electron gun in this case operated in the pulse regime. The pulse signal was delivered to the entrance of the time-amplitude converter (c) and finally to the multichannel amplitude analyser (7). The time scale of the converter changed from 100 nsec to 10 mcsec. The electron gun for the temporal decay measurements was governed by the pulses from the generator (8) with the duration of 10-200 nsec, which were the start pulses of the time-amplitude converter.

For the Hanle technique measurements the electron gun operated continuosly. The magnetic field was applied by the Helmholtz coils (9) orthogonally to the direction of observation and the axis of the electron beam. The linear polarizer (10) was mounted in the optical channel and its axis was directed parallel to the electron beam. The magnetic field strength was changed periodically in a stepwise saw-tooth way with the period of 2.5 sec. Such a signal was formed by the special signal processing unit (II) and was amplified by the power amplifier (12). The same

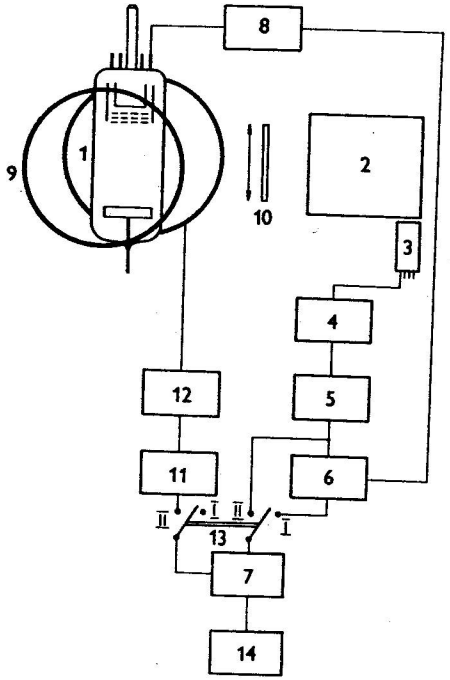

Fig. 4. Scheme of the complex τ-metric set up on the basis of the electron gun.

unit (II) realized the switching of the cells in the memory of the pulse analyser (7) which operated in this case at the synchronic storage regime. Hence every instantaneous magnetic field strength value H_n was connected rigidly to the nth memory address in the pulse analyser (7). For the Hanle technique the pulse signal from the discriminator (5) was delivered directly to the entrance of the pulse analyser (7).

By these means, the transfer from the temporal analysis of the spectral intensity decay to the Hanle effect measurements in this complex τ- metric set-up was made directly by the change of the switch (13) position I→II and the electron gun operating regime. The data were processed by a small computer (14).

IV. RESULTS AND DISCUSSIONS

The complex study by the delayed coincidence and the Hanle methods was performed for the $2p$- neon and some states of Kr11. The population decay curves

Table 1

Lifetimes τ (nsec) and the cascade shares for the $2p$ neon levels at the electron beam excitation with the energy 35 eV

Level	λ(nm)	τ'	τ^k	C(%)	τ_k (Hanle)	τ_k [1)]
$2p_5$	626.6	25 ± 3	115	14	19.5 ± 0.8	19.9 ± 0.4
$2p_6$	614.3	24 ± 2	175	10	19.1 ± 1.2	19.7 ± 0.2
$2p_9$	640.2	26 ± 4	273	13	18.0 ± 0.6	19.4 ± 0.6

[1)] Bennet , W.R., Kindlmann , P.J.: Phys. Rev. *149* (1966), 38

for the neon $2p_5$, $2p_6$, $2p_9$ levels showed the strong cascade transitions under different energy of the exciting electrons exceeding the excitation potential of the upper level. The attempt of the expansion of these decay curves on the different exponents led to the apparent τ_k values which exceeded significantly the same values obtained in [1] under the threshold electron impact excitation (see Table 1). In the Table 1 we denoted τ' as the apparent lifetime of the k level obtained for the two-exponential decay model τ^k as the effective decay constant of the cascade component, C as the share of the λ_{ik} spectral line intensity caused by the cascade component, $C = A_{jk}/(\gamma_k - \gamma_j)$. The estimate of the cascade share C was made by the resolution of the decay curve for the excitation electron energy 30 eV and the pulse duration of 20 nsec. It was found to be rather high (10-15%) and we supposed that the multicascade case takes place for the neon $2p$-states. The lifetime determination making use of the complex decay curves appeared to be a difficult problem. To get the accurate τ_k value we increased a number of the cascade components in the decay model and this decreased the difference between the measured lifetime and the threshold value, although these values still remained unequal [10]. A special study of the decay kinetics of the neon level $2p_9$ performed in [3] indicated that the complete decay model of this state under the electron energy exceeding the threshold energy comprises 13 cascade channels. Therefore the accurate study of the temporal characteristics of the excited states by the delayed coincidence technique under the nonthreshold conditions with an account for the cascade processes is a rather difficult problem.

The same $2p$ - states were studied by the Hanle technique for the energy of beam electrons exceeding the excitation potential of $2p$ - levels.

Taking into consideration that the effective decay time constant of the highly excited levels estimated by the delayed coincidence method was about 100 - 200 nsec (see Table 1), the Hanle signal shape of $2p$ neon level did not show any visible cascade distortions and appeared to be cascade-free (Fig. 5).

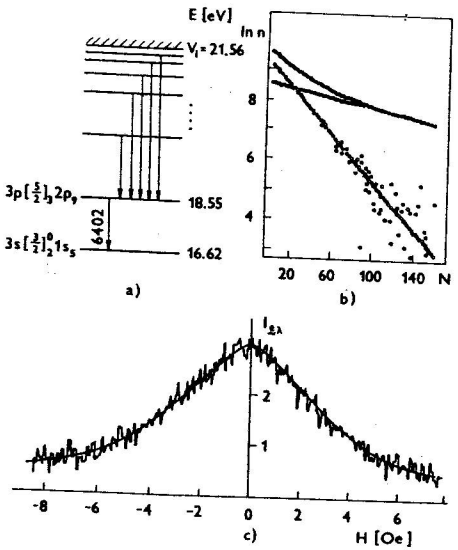

Fig. 5. Cascade transitions (a), decay curve (E=30eV;P_{Ne}=115 mTorr) (b); Hanle signal shape (E=30eV,P_{Ne}=8mTorr) (c); for the $2p_9$ neon level (λ=6402Å).

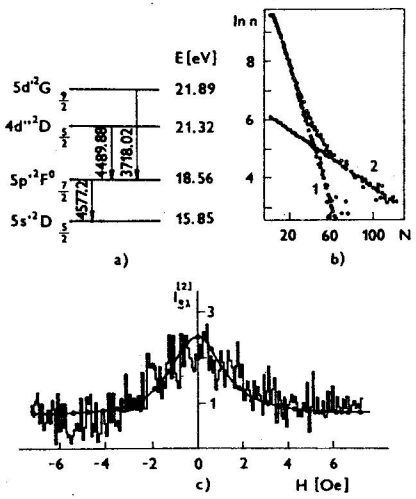

Fig. 6. Cascade picture for the Kr11 level $5p'^2F^0$(a), decay curve of the line 4577 Å(E=34 eV, P_{Kr}=50 mTorr) (b): 1 the decay component of the $5p'^2F^0$ level, 2 the cascade decay component, the cascade Hanle signal shape $I^{[2]}_{e\lambda}$ for the line 4577 Å at E=80 eV and P_{Kr}=30 mTorr (c) (points are theoretical).

The lifetimes measured directly using these signals without any cascade corrections were equal to the threshold delayed coincidence values (Table 1). We believe that in this case the total alignment cascading effect for many transition routes $I^{[2]}_{e\lambda}$ according to the formula (4) is small because of the compensation of the separate cascade contributions by each other.

A contrary cascade situation was observed investigating some of the Kr11 excited states. The decay curves of some levels obtained by the delayed coincidence method under non-threshold conditions were represented as a rule by a small number of exponential components. The graphical resolution of these decay curves with the help of the least square technique showed that the cascade share did not exceed 3-5% of the total level population at the electron energy 30 eV. The measured lifetimes were equal to the most reliable threshold values, which were obtained from the one-exponential population decay functions. The coincidence of the measured lifetimes with the results of the most reliable values indicated that chosen decay model correctly described our decay functions of the studied levels of Kr11 and the cascade parent levels (Fig. 6 a,b). The lifetime data of some Kr11 levels measured on a basis of these decay schemes are presented in Table 2. The accuracy of data is determined by the statistical scattering and the differential nonlinearity of the

experimental set-up. The errors of the lifetimes of highly excited cascade parent levels are determined entirely by the statistical scattering of data not exceeding 30%.

The Hanle signals for these states were also studied. The strong narrow Hanle signal components were observed, the width of which did not correspond to the natural width of the upper state of the studied transition. We explained the reason for these narrow components as the alignment cascade effect under the electron beam excitation.

This conclusion was supported by the fact that the general feature of the Kr11 cascade components were in accordance with the theoretical description of the phenomenon. The delayed coincidence study showed that in this case only a small number of cascade transitions exists (Fig. 6a) and its influence upon the Hanle signal shape even for the low cascade population shares (Table 2) may be high, because the cascade compensation in this case is not possible. The correlation between the intensities of the cascade components $I^{[2]}_{e\lambda}$ and the momenta of the cascade parent levels was noticed to be in accordance with our concept. Comparing the cascade situation for the Kr11 spectral lines 4355 Å(Fig. 6) and 4765 Å we see that $I^{[2]}_{e\lambda}$ (4765) is more than $I^{[2]}_{e\lambda}$ (4355), despite the higher cascade share for the

Table 2

Relative lifetimes (τ_k),decay constants of the cascade components (τ^k) and the cascade shares (C) for some KrII levels under the electron impact excitation with the energy 30 eV

Level	λ(nm)	τ_k (ns)	τ^k (ns)	C(%)	τ_k [1]	τ_k [2]	τ_k [3]
$5p^2P^0_{3/2}$	443.7	8.2 ± 0.6	75	0.9	8.49 ± 0.75		7.0
$5p^2D^0_{3/2}$	476.2	8.7 ± 0.7	69	1.2	8.69 ± 0.35	8.2 ± 0.5	6.6
$5p^2D^0_{5/2}$	461.9	8.3 ± 0.6	92	1.6	8.22 ± 0.33	8.0 ± 0.3	6.8
$5p^4S^0_{3/2}$	414.5	8.4 ± 0.7	104	1.4	8.31 ± 0.33		5.3
$5p^4D^0_{1/2}$	443.1	7.8 ± 0.6	72	2.5	8.12 ± 0.81		6.4
$5p^4D^0_{5/2}$	476.5	8.3 ± 0.7	137	2.2	10.18 ± 0.40		8.2
$5p^4D^0_{7/2}$	435.5	8.0 ± 0.8	75	5.6	7.70 ± 0.15	7.0 ± 0.7	6.1
$5p'^2F^0_{7/2}$	457.7	8.9 ± 0.9	43	3.2	8.35 ± 0.25	8.1 ± 0.5	7.1

[1] Donnely , K.E., Kindlman , P.J., Bennet , W.R.: JOSA *63* (1973), 1438.
[2] Fonseca , V., Campos , J.: J. Phys. B *15* (1982), 2349.
[3] Spector , N., Garpman , S.: JOSA *67* (1977), 155.

line 4355 Å(see Table 2). The cascade parent levels for the line 4355 Å have the momenta J_j=5/2, 7/2, 9/2 thus the partial cascade compensation of $I^{[2]}_{e\lambda}$ (4355) took place. For line 4765 Å J_j=7/2, 5/2, 3/2, all the cascade deposits (see formula (4) have the same signs and $I^{[2]}_{e\lambda}$ (4765) is much more pronounced. This idea is supported by the cascade effect for the lines 4619 Å and 4633 Å. Again the small cascade share but the favourable momenta of the cascade parent levels (ΔJ_j=0, ±2) give rise to the great magnitude of $I^{[2]}_{e\lambda}$, because the cascade polarization shares do not compensate each other.

The theoretical cascade Hanle profile $I^{[2]}_{e\lambda}$ was compared with the experimental signal for the KrII line 4577 Å(Fig. 6c). The relaxation constants of the cascade parent states measured by the delayed coincidence technique (Table 2) were used to calculate the cascade part of the Hanle profile $I^{[2]}_{e\lambda}$(H) with the help of the formula (4). We supposed that the population relaxation constant was close to the aligment relaxation constant for the low pressure range used in our work. The g_j - factors were obtained from the tables [9]. The comparison of the theoretical curve with the experimental Hanle signal profile (Fig. 6c) showed good agreement.

Our concept of the role of the cascade effect in different techniques of the lifetime determination and the influence of this effect on the resulting accuracy of the experimental data is also supported by the analysis of the independent experimental neon lifetime measurements (Table 3). The beam-foil excitation of atoms

Table 3

Values of mean lives of atomic levels in neon I.

Level	Mean life in nanoseconds				
	Beam-foil 1)	DC,electron beam	Hanle	DC,laser 4)	Theory 5)
$3p[1/2]_0$	25.4(7)	23(2) 2)	19.4(8) 3)	17.5(2)	15.2
$3p'[3/2]_2$	26.0(8)	22.5(10)	19.2(10) 6)	19.4(2)	17.3
$3p[3/2]_2$	28.9(9)	22(1)	18.2(7)	19.6(2)	19.8
$3p[5/2]_2$	27.8(8)	25.1(14) 7)	19.6(10)	20.6(3)	20
$3p[5/2]_3$	30.5(9)	24.0(15)	18.7(7)	19.2(3)	18.9
$3p[1/2]_1$	43.0(12)	26.3(15)	24.6(5)	25.9(4)	24.3
$3d[7/2]_3$			26(2) 8)		19.8
$3d[3/2]_2$			25(2)		19.5
$3d[3/2]_1$		7.25(60) 9)			8.29
$3d'[3/2]_1$		12.3(6)			12
$4d[3/2]_1$			21.5(20) 10)		17.7
$5d[3/2]_1$			37(7) 11)		34.7

[1] Denis , A., Desesquelles , J., Dufay , M.: Comp. rend. B *266* (1968), 1016.
[2] Klose , J.Z.: Phys. Rev. *141* (1966), 181.
[3] Gorny , M.B., Kazantsev , S.A., Matisov , B.G., Polezaeva , N.T.: Z. Phys. A *322* (1985), 25.
[4] Fujimoto , T., Goto , C., Fukuda , K.: Phys. Scr. *26* (1982), 443.
[5] Gruzdev , P.F., Loguinov , A.V.: Opt. and spektr. *45* (1978), 1050.
[6] Garrington , C.G.: Nucl. Instr. Meth. *110* (1973), 285.
[7] Osherovich , A.L., Verolainen , Ya.F.: Opt. and spektr. *22* (1967), 329.
[8] Kazantsev , S.A., Polzik , E.S.: Opt. and spektr. *41* (1976),1092.
[9] Lawrence , G.M., Liszt , H.S.: Phys. Rev. *178* (1969), 122.
[10] Kazantsev , S.A., Eiduk , V.I.: Opt. and spektr. *45* (1978), 858.
[11] Zhechev , D.Z.: Phys. Lett. (Franc.) *43* (1982), 67.

is known to induce all the possible cascade transitions with a maximum intensity. The data obtained by this method (see Table 3) exceed systematically the lifetimes measured by the delayed coincidence method with the selective laser excitation, by the Hanle method and theoretical values: The 3*p* level data obtained by the delayed coicidence method under the non-threshold election impact excitation also exceed the results of the same method under the selective laser excitation, the Hanle method and the theoretical results. On the other hand these values measured by the Hanle method, the delayed coincidence method under the selective layer excitation and the theoretical values are in good agreement. We are sure that these peculiarities confirm our idea that for many cascade routes the temporal decay method is mostly affected by the cascading in comparison with the Hanle

method, because of the cascade compensation of the total cascade share of the Hanle signal $I_{e\lambda}^{[2]}$.

A contrary relation between different experimental and theoretical lifetime values is typical for the highly excited nd neon states (see Table 3). For these states a better agreement between the theoretical and the delayed coincidence values takes place. But the results of the Hanle method for nd neon states are systematically greater. It is known that the number of the cascade transitions to the nd states is much less than to the np states.

So, the total cascade compensation of the cascade share of the Hanle signals for the nd states $I_{e\lambda}^{[2]}$ is impossible. The results of the delayed coincidence method for this case of the limited number of the cascade transitions are closer to the theoretical values than the same results of the Hanle method.

V. CONCLUSIONS

The neon and Kr11 complex lifetime measurements show that the role of the cascade effects in the delayed coincidence and the Hanle techniques is different. In the first method the radiative cascades for many cascade routes always strongly affect the decay curve and make the correct estimate of the decay curve distortions too difficult. Therefore the cascade errors of the measured lifetime in this case may be high. The resulting effect of the alignment cascade transfer depends on the number of cascade transitions, its relative contributions and momenta of the cascade parent levels. In the case of many cascade routes the cascade distortion of the Hanle signal may be small because of the compensation of cascade contributions by each other. We believe that apart from the development of the cascade-free methods the improvement of the experimental techniques founded on the electron impact excitation or the foil excitation will be of the complex use of the temperal decay and the coherent methods.

REFERENCES

[1] Bennet, W. R., Kindlmann, P. J.: Phys. Rev. *149* (1966), 38.
[2] Burstein, M. L., Nicolaich, A. Ya, Osherovich, A. L., Verolainen, Ya, F.: Pribory i Technika Experimenta (USSR) (1975), 210.
[3] Curtis, L. J., Schectman, R. M., Kohl, J. L., Chojnacki, D. A., Shoffstall, D. R.: Nucl Instrum. Meth. *90* (1970), 207.
[4] Ducloy, M., Dumont, M.: J. de Phys. *31* (1970), 419.
[5] Gorny, M. B., Kazantsev, S. A., Matisov, B. G., Polezhaeva, N. T.: Z. Phys. *A* 322 (1985), 25.
[6] Hanle, W.: Z. Phys. *30* (1924), 93.
[7] Kazantsev, S. A.: Abstracts 1 Europ. Conf. Atom. Phys. Heidelberg *5A* (1981), 535.
[8] Kazantsev, S. A.: Sov. Phys. Usp. *26(4)* (1983), 328.
[9] Moore, Ch.: *Atomic Energy Levels NBS Washington*, 1949.
[10] Osherovich, A. L., Verolainen, Ya, F.: Opt. Spectr. (USSR) *22* (1967), 329.
[11] Verolainen, Ya. F., Nicolaich, A. Ya.: Usp. Fiz. Nauk (USSR) *137* (1983), 305.

Received October 18th, 1990
Accepted for Publication January 11th, 1991

КАСКАДНЫЕ ЕФФЕКТЫ В ИЗМЕРЕНИИ ВРЕМЕН ЖИЗНИ

Обсуждаются каскадные еффекты в измерениях времени жизни. Теоретическое исследование и эксперименты, полученные с помощью комплексной τ-измерительной установки, показали, что роль каскадных еффектов в экспериментах по задержке совпадения и еффекта Ханле принципиально различны. Такие каскадные особенности можно использовать для в качестве дисперсии результатов, полученных с помощью различных экспериментальных методов.